

Clip Your Sequences Fairly: Enforcing Length Fairness for Sequence-Level RL

Hanyi Mao^{1*} Quanjia Xiao² Lei Pang² Haixiao Liu³

¹ University of Chicago ² Peking University ³ Duxiaoman

Abstract

We propose **FSPO** (Fair Sequence Policy Optimization), a sequence-level reinforcement learning method for LLMs that enforces length-fair clipping on the importance-sampling (IS) weight. We study RL methods with sequence-level IS and identify a mismatch when PPO/GRPO-style clipping is transplanted to sequences: a fixed clip range systematically reweights short vs. long responses, distorting the optimization direction. FSPO introduces a simple remedy: we clip the sequence log-IS ratio with a band that scales as \sqrt{L} . Theoretically, we formalize length fairness via a Length Reweighting Error (LRE) and prove that small LRE yields a cosine directional guarantee between the clipped and true updates. Empirically, FSPO flattens clip rates across length bins, stabilizes training, and outperforms baselines across model sizes and evaluation datasets, with the largest gains on the Qwen3-8B-Base model.

1 Introduction

Recent progress on reinforcement learning (RL) for large language models (LLMs) has been catalyzed by GRPO [21] and the broader RLVR paradigm [10], where rule-based, verifiable rewards are assigned to the entire response rather than token-wise signals. This framing has proven effective for improving mathematical reasoning and other verifiable tasks [3, 26, 27]. However, the optimization procedures used in current RLVR systems largely inherit token-level machinery from PPO-like methods [20], including the use of token-level importance-sampling (IS) ratios and token-level clipping. Meanwhile, subsequent works emphasize that once rewards are sequence-level, it is more faithful to operate with sequence-level IS so as to match the reward granularity [1, 31].

Despite the shift toward sequence-level IS, the theoretical distinctions and practical consequences of clipping in this setting remain underexplored. Existing sequence-level IS methods [1, 31] transplant the clipping mechanism from token-level methods directly and apply a *fixed* clip range to the probability ratio of the whole sequence. We argue that fixed sequence-level clipping is problematic: the dispersion of sequence-level *log* ratios increases with response length L . A fixed band therefore induces length-dependent acceptance rates and systematically reweights short versus long responses.

This paper studies sequence-level clipping through the lens of *length fairness*. We formalize a simple criterion: *acceptance rates should be approximately constant across response lengths*. We show that

*hanyim@uchicago.edu

fixed sequence-level clipping violates this criterion and can distort the training target. To address this, we propose **FSPO** (Fair Sequence Policy Optimization). FSPO preserves IS semantics and restores length fairness by using a \sqrt{L} -scaled acceptance band on the sequence log-ratio, which approximately equalizes acceptance across lengths.

To ground our analysis, we evaluate **FSPO** on sequence-level RL for mathematical reasoning. We compare against two sequence-level baselines: (i) *RLOO* with sequence-level IS and a fixed clip on the full-sequence ratio, and (ii) *GSPO* with ratio normalization. We report Avg@8 on MATH500, Avg@32 on AIME24 and AIME25, alongside diagnostic plots that measure acceptance rate as a function of response length to verify length fairness. Across two base model scales, we observe flatter acceptance across length bins, more stable training dynamics, and improved task scores; full results and ablations are presented in Section 6.

Background on RL for LLMs and RLVR is provided in Appendix A, and a detailed justification for sequence-level IS weights in RLVR scenario is given in Appendix B.

2 Length Fairness and Length Reweighting Error (LRE)

Following the notation in Appendix A, define the sequence-level log importance ratio

$$S(y | x) = \log \pi_\theta(y | x) - \log \pi_{\theta_{\text{old}}}(y | x).$$

Let $L = \text{len}(y)$ and fix a length-indexed band $b_L > 0$. The acceptance event (unclipped) is defined as

$$\mathcal{A}_L = \{y \mid |S(y | x)| \leq b_L\}.$$

We define the length-conditional acceptance rate $q(L) = \Pr_{\pi_{\theta_{\text{old}}}}(\mathcal{A}_L \mid L)$, and the per-length contributions

$$\begin{aligned} g_L^* &= \mathbb{E}_{\pi_{\theta_{\text{old}}}} \left[\frac{\pi_\theta(y | x)}{\pi_{\theta_{\text{old}}}(y | x)} \nabla_\theta \log \pi_\theta(y | x) A(x, y) \mid L \right], \\ g_L^b &= \mathbb{E}_{\pi_{\theta_{\text{old}}}} \left[\frac{\pi_\theta(y | x)}{\pi_{\theta_{\text{old}}}(y | x)} \nabla_\theta \log \pi_\theta(y | x) A(x, y) \mid \mathcal{A}_L, L \right], \end{aligned}$$

so that the true policy gradient target and its clipped surrogate are

$$g^* = \mathbb{E}_L[g_L^*], \quad g^b = \mathbb{E}_L[q(L) g_L^b].$$

Definition 2.1 (Length Reweighting Error (LRE)). *Let $\bar{q} = \mathbb{E}[q(L)]$. Define*

$$\text{LRE} = \frac{1}{2} \mathbb{E} \left[\left| \frac{q(L)}{\bar{q}} - 1 \right| \right].$$

Small LRE means the acceptance rate is nearly constant across response lengths.

Let $\kappa = \frac{\mathbb{E}[\|g_L^*\|]}{\|g^*\|} \geq 1$, which captures the dispersion of per-length signal magnitude.

Assumption 2.1 (Bounded stratification). *There exists $\eta \in [0, 1)$ such that for all L ,*

$$\|g_L^b - g_L^*\| \leq \eta \|g_L^*\|.$$

This assumption states that clipping does not severely distort the target within each length stratum.

Assumption 2.2 (Bounded correlation). *The correlation between $|q(L) - \bar{q}|$ and $\|g_L^*\|$ is mild so that*

$$\mathbb{E}[|q(L) - \bar{q}| \|g_L^*\|] \leq \gamma \mathbb{E}[|q(L) - \bar{q}|] \mathbb{E}[\|g_L^*\|].$$

This assumption is optional; see Appendix C.

Theorem 2.1 (Directional guarantee under length fairness). *Under Assumptions 2.1 and 2.2,*

$$\cos \angle(g^b, g^*) \geq \frac{1-\rho}{1+\rho}, \quad \rho \leq \kappa(\eta + 2\gamma(1+\eta) \text{LRE}).$$

The theorem implies that smaller LRE yields a larger lower bound on the cosine similarity between the clipped update and the true update. The proof and further discussion are provided in Appendix C.

3 Distribution of Sequence-Level Log Ratio

In this section we study the distribution of the sequence-level log importance-sampling (IS) ratio and derive practical guidance for designing procedures that achieve the *length fairness* criterion introduced earlier.

We view decoding under an LLM π with a limited context window K as a finite-state Markov chain on V^K , where V is the vocabulary; this reduction for autoregressive language models is discussed by Zekri et al. [30] in detail. Under randomized sampling with nonzero temperature, the chain is irreducible and aperiodic. Therefore, the Markov CLT for additive functionals [6, 14] applies to

$$S_L = \sum_{t \leq L} \log \frac{\pi_\theta(y_t | h_t)}{\pi_{\theta_{\text{old}}}(y_t | h_t)},$$

which yields the following theorem:

Theorem 3.1 (Gaussianity of the sequence-level log ratio). *The sequence log-IS ratio obeys an asymptotically Gaussian law:*

$$\frac{S_L - \mu_L}{\sqrt{L}} \Rightarrow \mathcal{N}(0, \sigma^2), \quad \mu_L = \text{theta}(L), \quad \sigma^2 > 0.$$

Figure 1 illustrates the empirical distribution of the sequence-level log IS ratio using all steps across the full training run. Consistent with the theorem, the empirical standard deviation of S_L grows approximately $\propto \sqrt{L}$. The observed estimator is $\hat{\sigma} = 0.0304$.

To further assess normality, we compute the standardized statistic

$$\hat{Z} = \frac{S_L - \hat{\mu}_L}{\sqrt{L} \hat{\sigma}},$$

where $\hat{\mu}_L$ is computed within each length bin and $\hat{\sigma}$ is estimated from all values of $(S_L - \hat{\mu}_L)/\sqrt{L}$. The Q-Q plot (right panel) shows that the fitted line coincides with the $y = x$ reference; the

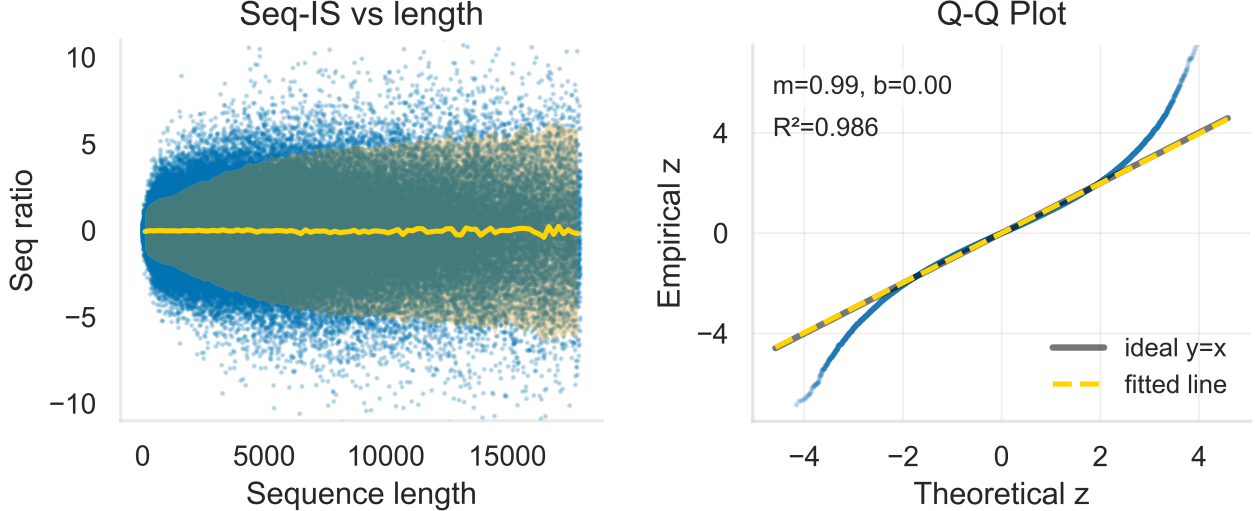


Figure 1: Empirical analysis of the sequence-level IS ratio. Sample size $n = 217,454$. **Left:** Empirical distribution of S_L . The yellow line shows the empirical mean and the shaded band the ± 2 empirical standard deviation, computed with a bin size of 200 (see Appendix C for justification of binning). **Right:** Q–Q plot testing normality. The sorted data point quantiles are shown in blue dots. We report the slope m , intercept b , and R^2 of the fitted line.

empirical distribution exhibits slightly heavier tails, but within ± 2 standard deviations it is very close to normal.

In Figure 1 (left), the estimated per-length mean $\hat{\mu}_L$ exhibits slightly larger fluctuations at larger lengths but remains small relative to $\hat{\sigma}$, thus empirically we set $\hat{\mu}_L \approx 0$.

Theoretical clip-fraction patterns of RLOO and GSPO. By Theorem 3.1, $S_L \approx \mathcal{N}(\mu_L, \sigma^2 L)$. Let $\Phi(\cdot)$ be the standard normal CDF. Similar to the acceptance-rate notation $q(L)$ used in Section 2, We denote the *clip probability* by $c(L) := 1 - q(L)$. For a symmetric two-sided clip in log space:

$$\text{RLOO: } c_{\text{RLOO}}(L) = \Pr(|S_L| > \xi) = 2\Phi\left(-\frac{\xi - \mu_L}{\sigma\sqrt{L}}\right) \approx 2\Phi\left(-\frac{\xi}{\sigma\sqrt{L}}\right), \quad (1)$$

$$\text{GSPO: } c_{\text{GSPO}}(L) = \Pr(|S_L| > \xi L) = 2\Phi\left(-\frac{\xi L - \mu_L}{\sigma\sqrt{L}}\right) \approx 2\Phi\left(-\frac{\xi\sqrt{L}}{\sigma}\right), \quad (2)$$

where the approximations use the empirically small drift $\mu_L \approx 0$. Both schemes induce clip probabilities that vary systematically with L .

To obtain a *constant* (length-independent) clip probability, **FSCO** sets $b_L = \mu_L + z\sigma\sqrt{L}$. With the same calculation as in Equations (1) and (2), we obtain

$$c_{\text{FSCO}}(L) \approx 2\Phi(-z),$$

which is independent of L and hence preserves the length fairness required by Theorem 2.1. Moreover, as suggested by the Q–Q plot in Figure 1 (right), choosing $z < 2$ keeps us in a regime where the normal approximation is highly accurate.

We plot the theoretical clip–probability curves in Figure 2, together with the empirically observed clip fractions, showing close agreement with the theory.

4 Method: FSPO

For each prompt $x \sim \mathcal{D}$ we sample G completions $\{y_i\}_{i=1}^G \sim \pi_{\theta_{\text{old}}}(\cdot | x)$ and optimize the PPO-style pessimistic surrogate

$$\mathcal{J}_{\text{FSPO}}(\theta) = \mathbb{E}_{x, \{y_i\}} \left[\frac{1}{G} \sum_{i=1}^G \min \left\{ \exp(S_\theta(y_i | x)) \hat{A}_i, \exp(\text{clip}(S_\theta(y_i | x), -b_{L_i}, b_{L_i})) \hat{A}_i \right\} \right], \quad (3)$$

where \hat{A}_i is an advantage estimate and $\text{clip}(s, \ell, u) = \min\{\max\{s, \ell\}, u\}$. The sequence-level log importance ratio is

$$S_\theta(y_i | x) = \log \frac{\pi_\theta(y_i | x)}{\pi_{\theta_{\text{old}}}(y_i | x)} = \sum_{t=1}^{L_i} \log \frac{\pi_\theta(y_{i,t} | h_{i,t})}{\pi_{\theta_{\text{old}}}(y_{i,t} | h_{i,t})}, \quad (4)$$

with $L_i = \text{len}(y_i)$ and $h_{i,t} = (x, y_{i,<t})$ the prefix at step t . FSPO performs *log-space* clipping by truncating S_θ to $[-b_L, b_L]$ before exponentiation, using the band as discussed in [Section 3](#)

$$b_L = \underbrace{\hat{\mu}_L}_{\text{drift}} + \underbrace{z\hat{\sigma}\sqrt{L}}_{\text{scale}}. \quad (5)$$

Note that in [Equation \(3\)](#) we average over the number of sequences G . This is natural for token-level clipping, but at sequence-level clipping is applied to the entire sequence and the clip fraction is typically much larger. A natural idea would be to exclude clipped sequences from the average. However, we keep G as the denominator, which serves as a dynamic step-size adjustment: when the clip fraction is higher which indicates that current mini-batch is unstable with higher variance, keeping the denominator at G correspondingly yields a smaller effectivem update for that batch.

Drift term. Following [Section 3](#), we set $\hat{\mu} = 0$. We empirically validate this simple setting flattens the clipping fraction and improves performance. In fact, the drift connects to token-level KLs:

$$\mathbb{E}_{\pi_{\theta_{\text{old}}}}[S_L] = \mathbb{E}_{\pi_{\theta_{\text{old}}}} \left[\sum_{t=1}^L \log \frac{\pi_\theta(y_t | h_t)}{\pi_{\theta_{\text{old}}}(y_t | h_t)} \right] = \sum_{t=1}^L -\text{KL}(\pi_{\theta_{\text{old}}}(\cdot | h_t) \| \pi_\theta(\cdot | h_t)). \quad (6)$$

This further justifies our setting of $\hat{\mu} = 0$, as we observe the KL between old and new policies is very small. However, this might not hold true for experimental settings significantly different than ours, in which cases a refined drift treatment could leverage [\(6\)](#); we leave this for future work.

Scale term. In [\(5\)](#), z controls the target clip fraction ([Section 3](#)), while $\hat{\sigma}$ is tracked by a running estimator over recent batches. In practice we set $c := z\hat{\sigma}$ and tune c as a single hyperparameter. A natural extension is to use asymmetric scales c_{upper} and c_{lower} , allowing separate control of the upper and lower clip ranges as in Yu et al. [\[29\]](#). Current RL implementations commonly include *dual-clip* [\[28\]](#), which effectively clips the ratio at $(1 + \epsilon_{\text{dual}})$ when $A < 0$; in our experiments, we also implement dual-clip in log-space and tune c_{dual} . Implementation details and discussion on hyperparameter tuning are provided in [Section D.2](#).

Compatibility with other components FSPO is a lightweight, plug-in modification that only changes the importance-ratio term in the policy loss. To isolate its effect, our implementation keeps all remaining components identical to the baselines (e.g., GRPO-style advantage). FSPO is compatible with alternative advantage estimators (e.g., \hat{A}^{LOO} [\[8, 12\]](#)), data filtering [\[29\]](#), and overlength penalties [\[29\]](#), among others.

5 Experimental Setup

5.1 Models and data.

We evaluate our method on two base LLMs: **Qwen3-1.7B-Base** and **Qwen3-8B-Base** [24]. For training, we use DAPO-Math-17K [29] together with AIME problems up to and including 2023 [13], accessed from [25]. Evaluation is conducted on held-out math benchmarks: MATH500 [4], AIME24 [15], and AIME25 [16]. We did not include MATH500 training set as we argue that its difficulty is inadequate for efficient training. We report **Avg@8** (per-sample accuracy averaged over 8 sampled completions) on MATH500, and **Avg@32** on AIME24/AIME25, since each AIME set contains only 30 questions and **Avg@32** yields more stable estimates. The detailed sampling configurations of evaluation process are provided in Appendix D.

5.2 Training framework.

We build on VERL [22] with vLLM [9] as roll-out backend and Megatron-LM [23] as training backend. All models are trained under identical sampling policies, batch sizes, and total token budgets. Complete hyperparameters and infrastructure details are provided in Appendix D.

5.3 Baselines.

We compare against sequence-level RL baselines: **RLOO**, **GSPO**, and our **FSPO**. We also include **GRPO** as an important baseline to highlight the advantages of sequence-level importance sampling when properly designed. All methods share the same data, sampling configuration, batch size, and number of training steps; FSPO differs only in employing log-space clipping with a length-scaled band. For the **RLOO** baseline, we adopt the policy-loss formulation described in Appendix A, but we use the GRPO-style advantage \hat{A}^{GRPO} rather than \hat{A}^{LOO} for a fair comparison with the other three methods.

6 Results and Analysis

6.1 Main Results

Section 6.1 reports results on MATH500 (Avg@8) and AIME24/25 (Avg@32) for two base model sizes. For each method we show the *best* checkpoint (peak score across saved checkpoints) and the *last* checkpoint (checkpoint of the last step). Overall, **FSPO** delivers consistent gains, with the largest margins on the harder AIME benchmarks and larger model size.

On **Qwen3-1.7B-Base**, **FSPO** attains the best AIME24 score (10.83/10.83) and the best last-average overall (29.16). On **Qwen3-8B-Base**, **FSPO** consistently outperforms the other methods across all benchmarks, achieving best/last averages of **49.79/48.98**, surpassing GRPO (+2.13/+1.93), RLOO (+1.99/+2.84), and GSPO (+2.82/+2.15). Gains are most pronounced on the more challenging AIME24 and AIME25: On AIME24, FSPO reaches **34.48/34.06**, yielding sizable gains versus GRPO (+3.23/+3.02), RLOO (+2.29/+4.06), and GSPO (+4.27/+3.85). On AIME25,

FSPO achieves **24.69/24.69**, outperforming GRPO (+1.77/+2.19), RLOO (+1.67/+3.86), and GSPO (+2.19/+2.61).

Overall, gains of FSPO grow with model scale and task difficulty. This is expected as larger models and harder tasks induce broader, more heterogeneous response-length distributions, a regime where **FSPO**’s length-fair clipping yields the largest benefits.

Method	MATH500 (Best/Last)	AIME24 (Best/Last)	AIME25 (Best/Last)	Average (Best/Last)
Qwen3-1.7B-Base				
base	52.20	3.02	3.33	19.52
GRPO	66.80/66.20	9.17/7.71	5.21/5.21	27.06/26.37
RLOO	70.80/70.80	10.73/7.60	6.77/6.77	29.43/28.39
GSPO	69.00/69.00	9.48/9.48	6.04/6.04	28.17/28.17
FSPO (ours)	70.20/70.20	10.83/10.83	6.46/6.46	29.16/ 29.16
Qwen3-8B-Base				
base	71.20	10.00	10.00	30.40
GRPO	88.80/87.60	31.25/31.04	22.92/22.50	47.66/47.05
RLOO	88.20/87.60	32.19/30.00	23.02/20.83	47.80/46.14
GSPO	88.20/ 88.20	30.21/30.21	22.50/22.08	46.97/46.83
FSPO (ours)	90.20/88.20	34.48/34.06	24.69/24.69	49.79/48.98

Table 1: Performance across benchmarks. "base" indicates the performance of the starting base model without RL training. MATH500 uses Avg@8; AIME24/AIME25 use Avg@32. Each cell shows **Best/Last** results. Bold indicates the best within each column.

6.2 Length-Fairness Diagnostics

We examine the clip fraction as a function of response length and compare the theoretical curve $c(L)$ predicted by (1) and 2; see Figure 2. The observed clip fractions match the theoretical patterns, where **RLOO** clips more frequently as length increases especially on short to medium lengths, **GSPO** shows a clear decreasing trend with length, and **FSPO** remains comparatively flat across lengths. Slightly higher values in the shortest-length bins in FSPO are due to limited samples and occasional outliers of abnormally short sequences.

The scale gap between the theoretical and empirical curves is expected due to the asymmetry between the upper and lower clip ranges in implementation and the skew of positive vs. negative advantages: PPO’s pessimistic min surrogate effectively upper-bounds clipping for positive-advantage samples only (and vice versa).

For LRE, we compute the *acceptance rate* $q(L) = 1 - c(L)$ and exclude anomalously short cases with $L < 1000$. The resulting LREs are 0.162 for RLOO, 0.264 for GSPO, and 0.037 for FSPO, where FSPO achieves the smallest LRE, according with its best performance demonstrated in 8B experiments.

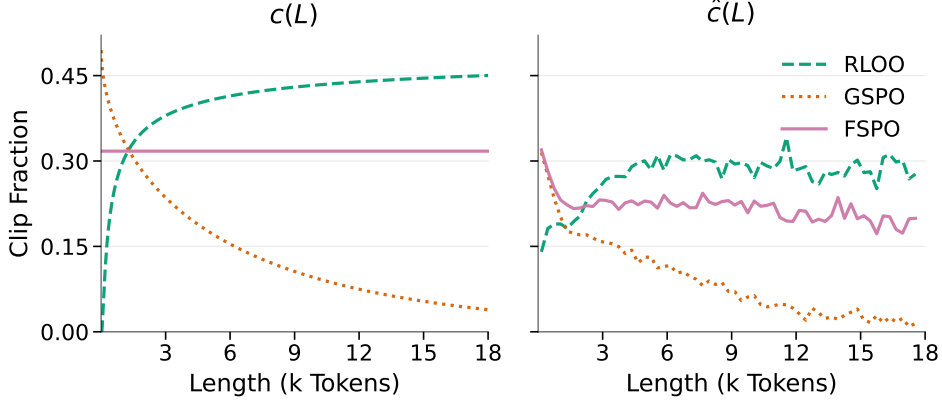


Figure 2: Theoretical and empirical clip fraction. **Left:** Theoretical clip probability $c(L)$ computed from Equations (1) and (2) using the hyperparameters in Appendix D.2, where we set $\xi = \log(1 + c_{\text{upper}})$. **Right:** Observed clip fraction $\hat{c}(L)$ with bin size = 200, collected from the experiments on Qwen3-8B-Base model.

6.3 Effectiveness: Learning Dynamics and Length Stability

As shown in Figure 3, both RLOO and FSPO learn quickly and increase response length early in training. However, RLOO’s response length later explodes to very large values, with much of the additional content being filler. A plausible explanation is that longer sequences are more likely to be clipped under RLOO; consequently, negative signals from long incorrect answers are suppressed, and the model fails to regulate length. Moreover, as responses grow longer, RLOO’s higher clip probability hampers learning and reward improvements plateau, whereas FSPO continues to make steady gains. By contrast, GSPO learns more slowly at the beginning and struggles to increase length, especially for the 1.7B model. On the 8B model, GSPO attains high rewards near or comparable to FSPO during training, yet its evaluation performance is suboptimal, indicating that length imbalance during training can impair calibration during generalization evaluation. FSPO attains the best performance with moderate average length on the 8B model, suggesting more balanced learning across lengths and more effective use of length.

To further assess downstream behavior, we report the *overlong rate* (the proportion of samples that reach the maximum response length and are truncated) and mean response length after excluding overlong samples. FSPO exhibits a markedly lower overlong rate, indicating stable control of response length. In contrast, methods with incorrect importance weights (GRPO, GSPO) show substantially higher overlong rates, while their mean lengths after excluding overlong samples are slightly lower, suggesting poor length allocation: responses tend to be either too long or too short, leading to suboptimal behavior. RLOO displays both higher overlong rate and larger length.

6.4 Ablation study: Larger Clip Range

As in Figure 2, RLOO’s clip fraction is large, potentially due to its relatively small clip range (Appendix D.2). Note that in FSPO the *ratio-level* clip range for a sequence with $L = 10,000$ is $\exp(\sqrt{10000} \times 0.03) = 20.09$, much larger than the $1.667(1 + c_{\text{upper}})$ used in RLOO. Thus, one may hypothesize that FSPO’s gains stem from being more permissive on long sequences than RLOO. To disentangle this, we evaluate RLOO with a *fixed* larger clip range (upper = 20, lower = 0.95). As

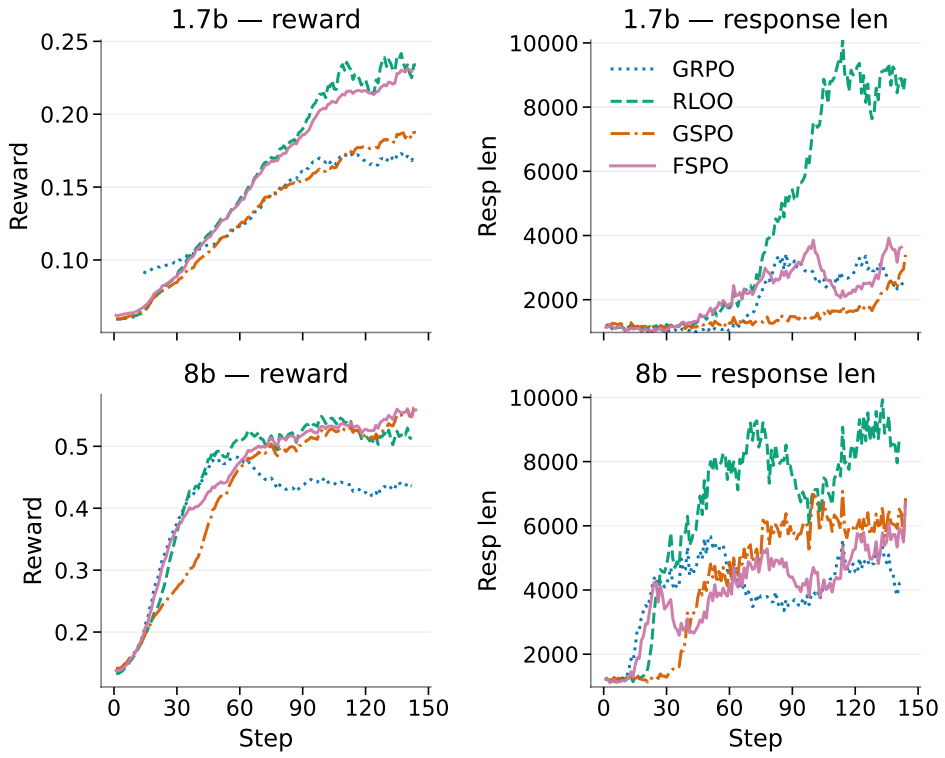


Figure 3: Learning dynamics during training. Left column: mean reward (1.7B and 8B). Right column: mean response length (1.7B and 8B). Reward curves are smoothed with EMA for visualization.

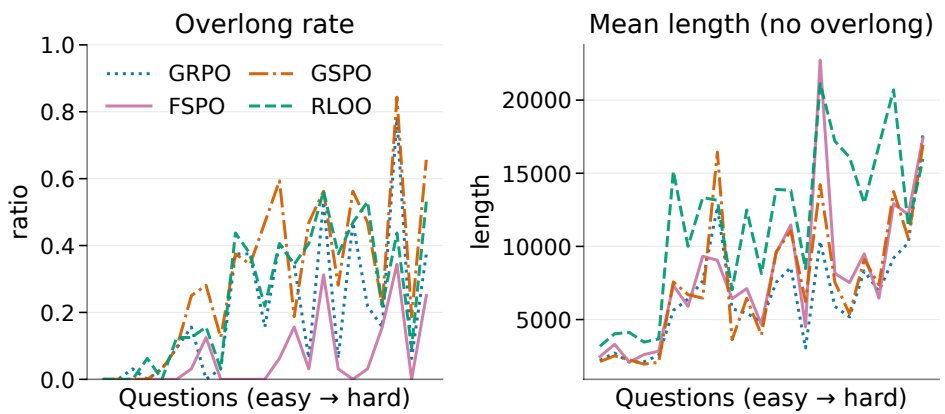


Figure 4: Overlong rate and mean response length on AIME24. We plot evaluation-time sampling; the x-axis orders the 30 problems from easy to hard, where difficulty is measured by the overall average accuracy across the four methods.

shown in Figure 5, this variant does not improve performance and can even be worse than standard RLOO. This indicates that *length fairness*, rather than mere leniency toward long responses, is key to FSPO’s effectiveness.

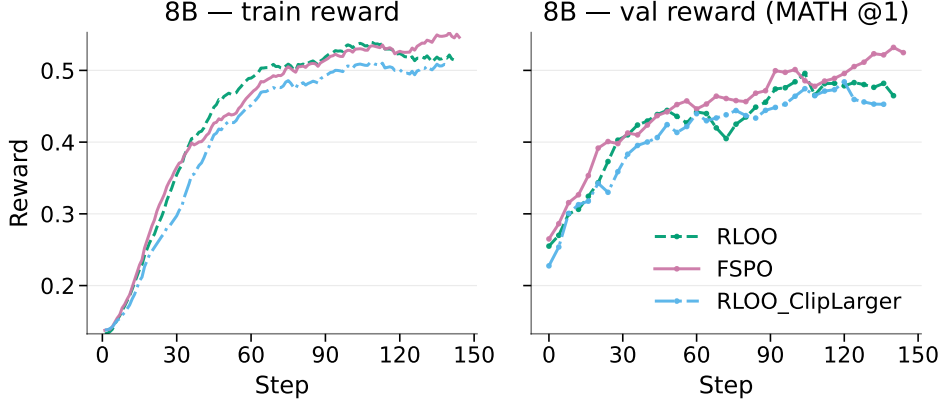


Figure 5: Ablation: fixed larger clip range. **Left:** mean rewards during training. **Right:** validation curves during training.

7 Conclusion

We studied the clipping mechanism in sequence-level importance sampling (IS) for RLVR scenarios, showing that a fixed clip range induces a length-reweighting pathology that biases acceptance across response lengths and distorts the effective objective. We formalized *length fairness* via the Length Reweighting Error (LRE) and established a cosine-direction guarantee linking small LRE to update-direction fidelity. Guided by an approximate Gaussian law for the sequence log-IS sum, we proposed **FSPO**: clipping in log-IS space with a \sqrt{L} -scaled band that preserves IS semantics while equalizing acceptance across lengths. Empirically, on three math benchmarks and two model scales, FSPO flattens acceptance-by-length and delivers consistent gains, with the largest improvements on the 8B model. Looking ahead, we will extend evaluation to other RLVR settings (e.g. code, tool-use, etc.), develop and evaluate adaptive clip-range schedules, and combine FSPO with stronger advantage estimation to build more capable RL pipelines.

References

- [1] Arash Ahmadian, Chris Cremer, Matthias Gallé, Marzieh Fadaee, Julia Kreutzer, Olivier Pietquin, Ahmet Üstün, and Sara Hooker. Back to basics: Revisiting reinforce style optimization for learning from human feedback in llms, 2024. URL <https://arxiv.org/abs/2402.14740>.
- [2] OpenCompass Contributors. Opencompass: A universal evaluation platform for foundation models. <https://github.com/open-compass/opencompass>, 2023.
- [3] DeepSeek-AI, Daya Guo, Dejian Yang, Haowei Zhang, Junxiao Song, Ruoyu Zhang, Runxin Xu, Qihao Zhu, Shirong Ma, Peiyi Wang, Xiao Bi, Xiaokang Zhang, Xingkai Yu, Yu Wu, Z. F. Wu, Zhibin Gou, Zhihong Shao, Zhuoshu Li, Ziyi Gao, Aixin Liu, Bing Xue, Bingxuan Wang, Bochao Wu, Bei Feng, Chengda Lu, Chenggang Zhao, Chengqi Deng, Chenyu Zhang, Chong Ruan, Damai Dai, Deli Chen, Dongjie Ji, Erhang Li, Fangyun Lin, Fucong Dai, Fuli Luo, Guangbo Hao, Guanting Chen, Guowei Li, H. Zhang, Han Bao, Hanwei Xu, Haocheng Wang, Honghui Ding, Huajian Xin, Huazuo Gao, Hui Qu, Hui Li, Jianzhong Guo, Jiashi Li, Jiawei Wang, Jingchang Chen, Jingyang Yuan, Junjie Qiu, Junlong Li, J. L. Cai, Jiaqi Ni, Jian Liang, Jin Chen, Kai Dong, Kai Hu, Kaige Gao, Kang Guan, Kexin Huang, Kuai Yu, Lean Wang, Lecong Zhang, Liang Zhao, Litong Wang, Liyue Zhang, Lei Xu, Leyi Xia, Mingchuan Zhang, Minghua Zhang, Minghui Tang, Meng Li, Miaojun Wang, Mingming Li, Ning Tian, Panpan Huang, Peng Zhang, Qiancheng Wang, Qinyu Chen, Qiushi Du, Ruiqi Ge, Ruisong Zhang, Ruizhe Pan, Runji Wang, R. J. Chen, R. L. Jin, Ruyi Chen, Shanghao Lu, Shangyan Zhou, Shanhua Chen, Shengfeng Ye, Shiyu Wang, Shuiping Yu, Shunfeng Zhou, Shuting Pan, S. S. Li, Shuang Zhou, Shaoqing Wu, Shengfeng Ye, Tao Yun, Tian Pei, Tianyu Sun, T. Wang, Wangding Zeng, Wanjia Zhao, Wen Liu, Wenfeng Liang, Wenjun Gao, Wenqin Yu, Wentao Zhang, W. L. Xiao, Wei An, Xiaodong Liu, Xiaohan Wang, Xiaokang Chen, Xiaotao Nie, Xin Cheng, Xin Liu, Xin Xie, Xingchao Liu, Xinyu Yang, Xinyuan Li, Xuecheng Su, Xuheng Lin, X. Q. Li, Xiangyue Jin, Xiaojin Shen, Xiaosha Chen, Xiaowen Sun, Xiaoxiang Wang, Xinnan Song, Xinyi Zhou, Xianzu Wang, Xinxia Shan, Y. K. Li, Y. Q. Wang, Y. X. Wei, Yang Zhang, Yanhong Xu, Yao Li, Yao Zhao, Yaofeng Sun, Yaohui Wang, Yi Yu, Yichao Zhang, Yifan Shi, Yiliang Xiong, Ying He, Yishi Piao, Yisong Wang, Yixuan Tan, Yiyang Ma, Yiyuan Liu, Yongqiang Guo, Yuan Ou, Yuduan Wang, Yue Gong, Yuheng Zou, Yujia He, Yunfan Xiong, Yuxiang Luo, Yuxiang You, Yuxuan Liu, Yuyang Zhou, Y. X. Zhu, Yanhong Xu, Yanping Huang, Yaohui Li, Yi Zheng, Yuchen Zhu, Yunxian Ma, Ying Tang, Yukun Zha, Yuting Yan, Z. Z. Ren, Zehui Ren, Zhangli Sha, Zhe Fu, Zhean Xu, Zhenda Xie, Zhengyan Zhang, Zhewen Hao, Zhicheng Ma, Zhigang Yan, Zhiyu Wu, Zihui Gu, Zijia Zhu, Zijun Liu, Zilin Li, Ziwei Xie, Ziyang Song, Zizheng Pan, Zhen Huang, Zhipeng Xu, Zhongyu Zhang, and Zhen Zhang. Deepseek-r1: Incentivizing reasoning capability in llms via reinforcement learning, 2025. URL <https://arxiv.org/abs/2501.12948>.
- [4] Dan Hendrycks, Collin Burns, Saurav Kadavath, Akul Arora, Steven Basart, Eric Tang, Dawn Song, and Jacob Steinhardt. Measuring mathematical problem solving with the math dataset, 2021. URL <https://arxiv.org/abs/2103.03874>.
- [5] Hugging Face TRL Team. Rloo trainer (trl documentation). https://huggingface.co/docs/trl/en/rloo_trainer, 2025. Accessed: 2025-09-09.

[6] Galin L. Jones. On the markov chain central limit theorem. *Probability Surveys*, 1:299–320, 2004. doi: 10.1214/154957804100000051. URL <https://projecteuclid.org/journals/probability-surveys/volume-1/issue-none/On-the-Markov-chain-central-limit-theorem/10.1214/154957804100000051.full>.

[7] Sham Kakade and John Langford. Approximately optimal approximate reinforcement learning. In *Proceedings of the 19th International Conference on Machine Learning (ICML 2002)*, pages 267–274, Sydney, Australia, 2002. Morgan Kaufmann.

[8] Wouter Kool, Herke van Hoof, and Max Welling. Buy 4 REINFORCE samples, get a baseline for free!, 2019. URL <https://openreview.net/forum?id=r1lgTGL5DE>.

[9] Woosuk Kwon, Zhuohan Li, Siyuan Zhuang, Ying Sheng, Lianmin Zheng, Cody Hao Yu, Joseph E. Gonzalez, Hao Zhang, and Ion Stoica. Efficient memory management for large language model serving with pagedattention. In *Proceedings of the ACM SIGOPS 29th Symposium on Operating Systems Principles*, 2023.

[10] Nathan Lambert, Jacob Morrison, Valentina Pyatkin, Shengyi Huang, Hamish Ivison, Faeze Brahman, Lester James V. Miranda, Alisa Liu, Nouha Dziri, Shane Lyu, Yuling Gu, Saumya Malik, Victoria Graf, Jena D. Hwang, Jiangjiang Yang, Ronan Le Bras, Øyvind Tafjord, Chris Wilhelm, Luca Soldaini, Noah A. Smith, Yizhong Wang, Pradeep Dasigi, and Hannaneh Hajishirzi. Tulu 3: Pushing frontiers in open language model post-training. *arXiv preprint arXiv:2411.15124*, 2025. doi: 10.48550/arXiv.2411.15124. URL <https://arxiv.org/abs/2411.15124>. Introduces RL with Verifiable Rewards (RLVR) and reports gains on math/instruction-following.

[11] Sergey Levine. Deep reinforcement learning, lecture 9: Policy gradient methods. Course lecture slides, CS 285: Deep Reinforcement Learning, 2019. URL <https://rail.eecs.berkeley.edu/deeprlcourse/deeprlcourse/static/slides/lec-9.pdf>. Accessed: 2025-09-14.

[12] Zichen Liu, Changyu Chen, Wenjun Li, Penghui Qi, Tianyu Pang, Chao Du, Wee Sun Lee, and Min Lin. Understanding r1-zero-like training: A critical perspective, 2025. URL <https://arxiv.org/abs/2503.20783>.

[13] Mathematical Association of America, American Mathematics Competitions. American invitational mathematics examination (aime): Problems (1983–2023). <https://maa.org/maa-invitational-competitions/>, 2024. Problems copyrighted by MAA AMC.

[14] Michael Maxwell and Michael Woodroffe. Central limit theorems for additive functionals of markov chains. *The Annals of Probability*, 28(2):713–724, 2000. doi: 10.1214/aop/1019160258. URL <https://projecteuclid.org/journals/annals-of-probability/volume-28/issue-2/Central-limit-theorems-for-additive-functionals-of-Markov-chains/10.1214/aop/1019160258.full>.

[15] Maxwell-Jia. Aime 2024 dataset. Dataset, 2025. URL https://huggingface.co/datasets/Maxwell-Jia/AIME_2024. MIT License.

[16] OpenCompass. Aime 2025 dataset. Dataset, 2025. URL <https://huggingface.co/datasets/opencompass/AIME2025>. MIT License.

[17] Long Ouyang, Jeff Wu, Xu Jiang, Diogo Almeida, Carroll L. Wainwright, Pamela Mishkin, Chong Zhang, Sandhini Agarwal, Katarina Slama, Alex Ray, John Schulman, Jacob Hilton, Fraser Kelton, Luke Miller, Maddie Simens, Amanda Askell, Peter Welinder, Paul Christiano, Jan Leike, and Ryan Lowe. Training language models to follow instructions with human feedback. In *NeurIPS*, 2022. URL https://proceedings.neurips.cc/paper_files/paper/2022/file/b1efde53be364a73914f58805a001731-Paper-Conference.pdf.

[18] John Schulman, Sergey Levine, Pieter Abbeel, Michael Jordan, and Philipp Moritz. Trust region policy optimization. In *Proceedings of the 32nd International Conference on Machine Learning (ICML)*, pages 1889–1897. PMLR, 2015. URL <https://proceedings.mlr.press/v37/schulman15.html>.

[19] John Schulman, Philipp Moritz, Sergey Levine, Michael Jordan, and Pieter Abbeel. High-dimensional continuous control using generalized advantage estimation, 2015. URL <https://arxiv.org/abs/1506.02438>.

[20] John Schulman, Filip Wolski, Prafulla Dhariwal, Alec Radford, and Oleg Klimov. Proximal policy optimization algorithms. *arXiv preprint arXiv:1707.06347*, 2017. URL <https://arxiv.org/abs/1707.06347>.

[21] Zhihong Shao, Peiyi Wang, Qihao Zhu, Runxin Xu, Junxiao Song, Xiao Bi, Haowei Zhang, Mingchuan Zhang, Y. K. Li, Y. Wu, and Daya Guo. Deepseekmath: Pushing the limits of mathematical reasoning in open language models. *arXiv preprint arXiv:2402.03300*, 2024. doi: 10.48550/arXiv.2402.03300. URL <https://arxiv.org/abs/2402.03300>.

[22] Guangming Sheng, Chi Zhang, Zilingfeng Ye, Xibin Wu, Wang Zhang, Ru Zhang, Yanghua Peng, Haibin Lin, and Chuan Wu. Hybridflow: A flexible and efficient rlhf framework. In *Proceedings of the Twentieth European Conference on Computer Systems, EuroSys ’25*, page 1279–1297. ACM, March 2025. doi: 10.1145/3689031.3696075. URL <http://dx.doi.org/10.1145/3689031.3696075>.

[23] Mohammad Shoeybi, Mostofa Patwary, Raul Puri, Patrick LeGresley, Jared Casper, and Bryan Catanzaro. Megatron-lm: Training multi-billion parameter language models using model parallelism. *arXiv preprint arXiv:1909.08053*, 2019.

[24] Qwen Team. Qwen3 technical report, 2025. URL <https://arxiv.org/abs/2505.09388>.

[25] Hemish Veeraboina. Aime problem set 1983-2024, 2024. URL <https://www.kaggle.com/datasets/hemishveeraboina/aime-problem-set-1983-2024>.

[26] Yiping Wang, Qing Yang, Zhiyuan Zeng, Liliang Ren, Liyuan Liu, Baolin Peng, Hao Cheng, Xuehai He, Kuan Wang, Jianfeng Gao, Weizhu Chen, Shuohang Wang, Simon Shaolei Du, and Yelong Shen. Reinforcement learning for reasoning in large language models with one training example. *arXiv preprint arXiv:2504.20571*, 2025. doi: 10.48550/arXiv.2504.20571. URL <https://arxiv.org/abs/2504.20571>.

[27] Xumeng Wen, Zihan Liu, Shun Zheng, Zhijian Xu, Shengyu Ye, Zhirong Wu, Xiao Liang, Yang Wang, Junjie Li, Ziming Miao, Jiang Bian, and Mao Yang. Reinforcement learning with verifiable rewards implicitly incentivizes correct reasoning in base llms. *arXiv preprint arXiv:2506.14245*, 2025. URL <https://arxiv.org/abs/2506.14245>.

- [28] Deheng Ye, Zhao Liu, Mingfei Sun, Bei Shi, Peilin Zhao, Hao Wu, Hongsheng Yu, Shaojie Yang, Xipeng Wu, Qingwei Guo, Qiaobo Chen, Yinyuting Yin, Hao Zhang, Tengfei Shi, Liang Wang, Qiang Fu, Wei Yang, and Lanxiao Huang. Mastering complex control in moba games with deep reinforcement learning, 2020. URL <https://arxiv.org/abs/1912.09729>.
- [29] Qiying Yu, Zheng Zhang, Ruofei Zhu, Yufeng Yuan, Xiaochen Zuo, Yu Yue, Weinan Dai, Tiantian Fan, Gaohong Liu, Lingjun Liu, Xin Liu, Haibin Lin, Zhiqi Lin, Bole Ma, Guangming Sheng, Yuxuan Tong, Chi Zhang, Mofan Zhang, Wang Zhang, Hang Zhu, Jinhua Zhu, Jiaze Chen, Jiangjie Chen, Chengyi Wang, Hongli Yu, Yuxuan Song, Xiangpeng Wei, Hao Zhou, Jingjing Liu, Wei-Ying Ma, Ya-Qin Zhang, Lin Yan, Mu Qiao, Yonghui Wu, and Mingxuan Wang. Dapo: An open-source llm reinforcement learning system at scale, 2025.
- [30] Oussama Zekri, Ambroise Odonnat, Abdelhakim Benechehab, Linus Bleistein, Nicolas Boullé, and Ievgen Redko. Large language models as markov chains, 2025. URL <https://arxiv.org/abs/2410.02724>.
- [31] Chujie Zheng, Shixuan Liu, Mingze Li, Xiong-Hui Chen, Bowen Yu, Chang Gao, Kai Dang, Yuqiong Liu, Rui Men, An Yang, Jingren Zhou, and Junyang Lin. Group sequence policy optimization. *arXiv preprint arXiv:2507.18071*, 2025. URL <https://arxiv.org/abs/2507.18071>.

A Preliminaries and Related Work

Setup. Let $x_i \in \mathcal{X}$ be a context (prompt) drawn from a data distribution $p(x)$, and let $y_i = (y_{i,1}, \dots, y_{i,|y_i|}) \in \mathcal{Y}$ be a response (a token sequence). Under a policy π_θ (which is an LLM in our setting), the outcome distribution is

$$\pi_\theta(y_i | x_i) = \prod_{t=1}^{|y_i|} \pi_\theta(y_{i,t} | h_{i,t}),$$

where $h_{i,t} = (x_i, y_{i,<t})$ is the previous state.

RLHF and PPO. Reinforcement Learning from Human Feedback (RLHF) [17] frames alignment as policy optimization against a reward model learned from human preference data. RLHF utilizes PPO [20] algorithm: it assigns reward signal to the last token and uses GAE [19] to compute per-token advantages $\hat{A}_{i,t}$. The typical PPO objective is

$$\mathcal{J}_{\text{PPO}}(\theta) = \frac{1}{N} \sum_{i=1}^N \frac{1}{|y_i|} \sum_{t=1}^{|y_i|} \min\left(r_{i,t}(\theta) \hat{A}_{i,t}, \text{clip}(r_{i,t}(\theta), 1 - \epsilon, 1 + \epsilon) \hat{A}_{i,t}\right), \quad (7)$$

where $r_{i,t}(\theta) = \frac{\pi_\theta(y_{i,t} | h_{i,t})}{\pi_{\theta_{\text{old}}}(y_{i,t} | h_{i,t})}$ is the token-level IS weight.

RLVR paradigm and GRPO. For math, programming and other verifiable tasks, recent systems adopt the RLVR [10] paradigm: rule-based, sequence-level rewards that can be automatically checked. Representative methods include GRPO [21], DAPO [29], DrGRPO [12], etc. A typical GRPO-style update draws a group of G completions $\{y_i\}_{i=1}^G$ for the same prompt x under $\pi_{\theta_{\text{old}}}$ (note here we abuse the notation of index i as within-group index, while previous i is the index in the dataset), computes sequence rewards $R_i = G(x, y_i)$, and uses the group mean as a baseline so that $\hat{A}_i = (R_i - \frac{1}{G} \sum_{j=1}^G R_j)/\sigma$, where σ is the standard deviation of rewards of this group. The advantage for each token is $\hat{A}_{i,t} = \hat{A}_i$ for all $t = 1, 2, \dots, |y_i|$. The objective of GRPO is similar to equation 7, thus inherits the token-level IS weight and clipping.

Sequence-level Importance Sampling Recent works argue that LLM RL with sequence rewards should be performed with sequence-level importance sampling (IS). RLOO [1] models LLM as a one-step bandit and treats a whole response as an action. According to the implementation of TRL RLOO_Trainer [5], the objective of RLOO is

$$\mathcal{J}_{\text{RLOO}}(\theta) = \mathbb{E}_{x, \{y_i\} \sim \pi_{\theta_{\text{old}}}} \left[\frac{1}{G} \sum_{i=1}^G \min\left(s_i(\theta) \hat{A}_i^{\text{LOO}}, \text{clip}(s_i(\theta), 1 - \epsilon, 1 + \epsilon) \hat{A}_i^{\text{LOO}}\right) \right], \quad (8)$$

where

$$s_i(\theta) = \frac{\pi_\theta(y_i | x_i)}{\pi_{\theta_{\text{old}}}(y_i | x_i)} \quad (9)$$

is the sequence-level IS weight which matches the reward granularity, and \hat{A}_i^{LOO} is the leave-one-out unbiased advantage estimator in [8]. A recent work GSPO [31] pursue the same goal of sequence-level IS but normalize the IS ratio by length (e.g., using $s_i^{\text{norm}} = \exp(\frac{1}{|y_i|} \log s_i)$) before clipping:

$$\mathcal{J}_{\text{GSPO}}(\theta) = \mathbb{E} \left[\frac{1}{G} \sum_{i=1}^G \min \left(s_i^{\text{norm}}(\theta) \hat{A}_i, \text{clip}(s_i^{\text{norm}}(\theta), 1 - \epsilon, 1 + \epsilon) \hat{A}_i \right) \right]. \quad (10)$$

The idea of normalization by length is out of a similar motivation of providing a same scale for different lengths [31]. However, we argue that this normalization does not reach the goal of balancing the clipping scale, and also undermines the correctness IS weights.

B Why Sequence-level IS for RLVR

RLOO [1] models the entire generation as a single action (a bandit setting), but its context is RLHF and it does not yet discuss the inadequacy of token-level IS and the correctness of sequence-level IS for RLVR. GSPO [31] notes that, in RLVR, the granularity of importance sampling should match the granularity of the reward, but it does not provide a detailed theoretical justification.

Here we offer a detailed and illuminating discussion. As proved by [7, 18] and presented in [11], the improvement of the objective between old and new parameters can be written as

$$J(\theta) - J(\theta_{\text{old}}) = \mathbb{E}_{\tau \sim \pi_\theta} \left[\sum_{t=0}^{\infty} \gamma^t A^{\pi_{\theta_{\text{old}}}}(s_t, a_t) \right] \quad (11)$$

$$= \sum_{t=0}^{\infty} \mathbb{E}_{s_t \sim p_\theta(s_t)} \left[\mathbb{E}_{a_t \sim \pi_\theta(a_t|s_t)} [\gamma^t A^{\pi_{\theta_{\text{old}}}}(s_t, a_t)] \right] \quad (12)$$

$$= \sum_{t=0}^{\infty} \mathbb{E}_{s_t \sim p_\theta(s_t)} \left[\mathbb{E}_{a_t \sim \pi_{\theta_{\text{old}}}(a_t|s_t)} \left[\frac{\pi_\theta(a_t|s_t)}{\pi_{\theta_{\text{old}}}(a_t|s_t)} \gamma^t A^{\pi_{\theta_{\text{old}}}}(s_t, a_t) \right] \right]. \quad (13)$$

This is where token-level importance sampling is introduced, as we need to express expectations under π_θ using samples sampled from θ_{old} in practice. Note that the state distribution $s_t \sim p_\theta(s_t)$ is not corrected by IS: $p(s_t)$ factors into a product over all previous actions, so naively correcting it can lead to high variance and poor estimates. In fact, the trust region in TRPO and the clipping mechanism in PPO are designed precisely to mitigate the mismatch incurred when estimating $s_t \sim p_\theta(s_t)$ using samples from $s_t \sim p_{\theta_{\text{old}}}(s_t)$, since one can show that $p_{\theta_{\text{old}}}(s_t)$ and $p_\theta(s_t)$ remain close when $\pi_{\theta_{\text{old}}}$ and π_θ are close.

However, this formulation becomes problematic in the RLVR setting, where all tokens in a sequence share a single advantage. From Equation (11) to Equation (12), the expectations over $(s_{t+1}, a_{t+1}, s_{t+2}, \dots)$ are marginalized out. That step requires the summand depends only on (s_t, a_t) and not on the *future* part of the trajectory. This condition fails in RLVR, in which $A(s_t, a_t) = A(\tau)$ for all t in a sample sequence.

To make this concrete, consider an imagined batch with two samples $y_a, y_b \sim \pi_{\theta_{\text{old}}}(y | x)$,

$$y_a = (y_0, y_1, \dots, y_t, y_{t+1}^{(a)}, y_{t+2}^{(a)}, \dots), \quad y_b = (y_0, y_1, \dots, y_t, y_{t+1}^{(b)}, y_{t+2}^{(b)}, \dots),$$

which share the same tokens up to index t and diverge from $t+1$ onward. Suppose y_a is correct and y_b is incorrect (e.g., $A(y_a) = 0.5$, $A(y_b) = -0.5$), $\pi_{\theta_{\text{old}}}(y_a) = \pi_{\theta_{\text{old}}}(y_b)$, and $\pi_\theta(y_a) > \pi_\theta(y_b)$. This

setting implies that, under the current policy π_θ , conditioned on the shared prefix (y_0, \dots, y_t) , y_a is more likely to occur than y_b , i.e., the model is more likely to answer correctly than incorrectly given the prefix. Intuitively, the next update should increase the likelihood of the prefix (y_0, \dots, y_t) . Sequence-level IS achieves this, because

$$\frac{\pi_\theta(y_a)}{\pi_{\theta_{\text{old}}}(y_a)} > \frac{\pi_\theta(y_b)}{\pi_{\theta_{\text{old}}}(y_b)},$$

and the shared-prefix gradients are accordingly weighted more for y_a than for y_b . By contrast, token-level IS assigns the same token-level ratios to the shared tokens (y_0, \dots, y_t) for both y_a and y_b (and for any other sample with that prefix), so it cannot express this desirable preference. This illustrates the advantage of sequence-level IS for RLVR.

Interestingly, in the case of sequence-level IS weight, the problem of $p_{\theta_{\text{old}}} \neq p_\theta$ as in PPO, TRPO does not hold, because the probability of the entire sequence is corrected. However, the clipping mechanism can be kept to solve the high-variance issue of sequence-level ratio and thus is still necessary.

C Proof of Theorem 2.1

Cosine lemma. For nonzero u, v , $\cos \angle(u, v) \geq \frac{\|v\| - \|u-v\|}{\|v\| + \|u-v\|}$.

Proof Note that $\cos \angle(g^b, g^*) = \cos \angle(g^b, \bar{q}g^*)$. To use cosine lemma, we want to bound $\|g^b - \bar{q}g^*\|$. Recall $g^b = \mathbb{E}_L[q(L)g_L^b]$, $g^* = \mathbb{E}_L[g_L^*]$, $\bar{q} = \mathbb{E}[q(L)]$. Decompose

$$g^b - \bar{q}g^* = \mathbb{E}_L[(q(L) - \bar{q})g_L^*] + \mathbb{E}_L[q(L)(g_L^b - g_L^*)].$$

We bound its norm as

$$\begin{aligned} \|g^b - \bar{q}g^*\| &\leq \underbrace{\mathbb{E}_L[|q(L) - \bar{q}|\|g_L^*\|]}_{\text{cross-length reweighting}} + \underbrace{\mathbb{E}_L[\|q(L)(g_L^b - g_L^*)\|]}_{\text{within-length stratification}} && \text{(by triangle inequality)} \\ &\leq \bar{q} \mathbb{E}_L \left[\left| \frac{q(L)}{\bar{q}} - 1 \right| \|g_L^*\| \right] + \eta \mathbb{E}_L [\|(q(L) - \bar{q})g_L^* + \bar{q}g_L^*\|] && \text{(by Assumption 2.1)} \\ &\leq (1 + \eta)\bar{q} \mathbb{E}_L \left[\left| \frac{q(L)}{\bar{q}} - 1 \right| \|g_L^*\| \right] + \eta\bar{q} \mathbb{E}_L [\|g_L^*\|] && \text{(by algebra)} \\ &\leq \bar{q} (2\gamma(1 + \eta) \text{LRE} + \eta) \mathbb{E}_L [\|g_L^*\|] && \text{(by Assumption 2.2 and definition of LRE)} \end{aligned}$$

Recall that $\mathbb{E}_L[\|g_L^*\|] = \kappa\|g^*\|$ and apply the cosine lemma with $u = g^b$, $v = \bar{q}g^*$, and Theorem 2.1 is proved.

Weighted-LRE variant If one wants to avoid any bounded co-variation concerns, define

$$\text{LRE}_w = \frac{1}{2} \mathbb{E} \left[\left| \frac{q(L)}{\bar{q}} - 1 \right| \frac{\|g_L^*\|}{\mathbb{E}\|g_L^*\|} \right].$$

Then the same argument yields the bound with LRE replaced by LRE_w .

More discussion: beyond length. It is worth noting that the proof of [Theorem 2.1](#) does not fundamentally rely on the specific choice of L as the partitioning variable. The argument only requires that the sample space can be partitioned into groups where (i) the signals across groups exhibit dispersion, and (ii) within-group stratification errors can be controlled. Thus, L can be replaced by any other reasonable attribute that induces such a partition, for example bins of lengths (which justifies the binning process in our diagnostic plots), or other salient structural features of the data. This perspective suggests a more general criterion for designing clipping mechanisms: it should not introduce systematic bias across groups of any reasonable partitioning attribute, unless such a bias is intentionally desired.

D Configurations

D.1 Training Configurations

We conduct experiments on a single $8 \times$ H200 (140 GB) GPUs. Under the configuration below, training for 1 epoch takes approximately 3–4 days; the wall-clock time grows with the average response length.

Table 2: Training configuration.

Item	Value
Prompt / Response max	2,000 / 18,000 tokens
Global batch size (sequences)	128
mini-batch	32
per-GPU micro-batch	32
total steps	144
Optimizer & LR	AdamW, 1×10^{-6}
Parallelism	Megatron TP=8
Rollout n	16
vLLM GPU-util	0.5
Seeds	42

D.2 Algorithmic Hyperparameters and Tuning

Limitation Due to compute constraints, we did not perform an exhaustive hyperparameter search. For settings similar to ours, we recommend fixing the base clipping scale c at 0.03 or higher. However, this value may not transfer across substantially different datasets or model sizes.

Interpreting c , z , and $\hat{\sigma}$ In our formulation, the sequence log-IS ratio S is clipped by a band whose width is

$$\text{band} = z \cdot \hat{\sigma}$$

Setting $c = 0.03$ is equivalent to choosing $z=1$ and $\hat{\sigma}=0.03$ in our environment (cf. [Sec. 3](#)). In our experiments we first obtain $\hat{\sigma}$ from a short baseline run, which inevitably introduces one preliminary pass.

To avoid a dedicated pilot run while preserving stability, we recommend:

1. Initialize with $z \in [1, 1.5]$ and a heuristic $\hat{\sigma}_0=0.03$ for warmup.
2. Maintain a running estimate $\hat{\sigma}_t$ of the log-IS ratio std via an exponential moving average (EMA): $\hat{\sigma}_t \leftarrow (1 - \alpha)\hat{\sigma}_{t-1} + \alpha \text{std}_{\text{batch}}(S)$.
3. Update the clip band as $z \cdot \hat{\sigma}_t$.

Table 3: Algorithmic hyperparameters

Hyperparameter	Value
Upper Clip c_{upper}	0.03
Lower Clip c_{lower}	0.03
Dual Clip c_{dual}	0.03
Loss aggregation	token-mean
use_KL	disabled
Entropy coefficient	0
Advantage Estimator	GRPO-style

Baseline Hyperparameters We also report the hyperparameters in our baseline implementations. Note that the clip-range here for baseline methods are in the ratio space as convention rather than the log space in our FSPO method. We adopt clip-higher as in [29] for GRPO, and follow the guidance in GSPO paper for GSPO. The cliprange_c hyperparameter is the parameter that VeRL uses to control dual-clip range.

Table 4: Baseline clipping configuration

Baseline	cliprange_upper	cliprange_lower	cliprange_dual
GRPO	0.28	0.2	3.0
RLOO	0.667	0.4	3.0
GSPO	4e-4	3e-4	disabled

D.3 Test-time Configurations

We use OpenCompass [2] as our evaluation framework.

Table 5: Decoding configuration

Item	Value
Temperature	0.6
Top- p	0.95
Top- k	200
Max generation tokens	32,000
Batch size	256
Tensor parallel	8
Data parallel	1